Kinetic studies of crystallization in mixtures of isotactic polystyrene and atactic polystyrene

Tetsuo Okada, Hiromu Saito and Takashi Inoue*
Department of Organic and Polymeric Materials, Tokyo Institute of Technology, Ookayama, Meguro-ku, Tokyo 152, Japan
(Received 12 July 1993; revised 2 May 1994)

We investigated the spherulite growth rate G in 60/40 isotactic polystyrene (i-PS)/atactic polystyrene (a-PS) mixtures under a polarized microscope with a TV video recording system. When the molecular weight M_A of a-PS was higher than 1.91×10^4, linear growth was observed, i.e. G was constant throughout the crystallization, and the chain diffusivity D_T decreased monotonously with increasing M_A. In contrast, when M_A was less than 5.2×10^3, the growth was non-linear, i.e. G decreased with time, and D_T increased with increasing M_A ($D_T \propto M_A^{1/2}$). Both M_A dependences on D_T were successfully interpreted using a modified Hoffman–Lauritzen theory involving the exclusion effect of a-PS. On the basis of this modified Hoffman–Lauritzen theory, the spherulite growth mode, i.e. linear or non-linear, was also interpreted in terms of a new kinetic parameter $\lambda = D_A^*/D_s$, D_a^* and D_s being the tracer diffusion coefficient of a-PS and the self-diffusion coefficient of i-PS, respectively.

(Keywords: polystyrene; blend; crystal growth rate)

INTRODUCTION

The spherulite growth kinetics in single-phase mixtures of crystalline and amorphous polymers have been described by the Hoffman–Lauritzen theory[1,2], taking into account the melting point depression and change in chain mobility with mixing. However, the crystallization behaviour in polymer mixtures essentially differs from that in neat polymer systems. In mixtures, exclusion of the amorphous component from the growth front would seriously affect the growth kinetics. The spherulite growth rate G in polymer/polymer mixtures is usually constant throughout the crystallization, i.e. linear growth seems to be general. On the other hand, in polymer/oligomer and polymer/solvent systems G often decreases with increasing crystallization time, i.e. non-linear growth occurs. Typical results are given in *Table 1*[3–7]. In the case of linear growth, the kinetics have been successfully described by a modified Hoffman–Lauritzen theory which is based on a two-step diffusion mechanism[4].

In this article we use the modified theory to interpret non-linearity. In the literature there are some results on the non-linearity of mixtures of isotactic polystyrene (i-PS) and atactic polystyrene (a-PS). In this paper we add such results, employing a series of a-PS specimens with a much wider range of molecular weights. Then we discuss the issue of non-linearity to uncover a quantitative criterion for non-linear growth.

* To whom correspondence should be addressed

EXPERIMENTAL

The isotactic polystyrene (i-PS) used in this study was purchased from General Science corporation. Atactic polystyrene (a-PS) samples were supplied by TOSOH Corporation. The a-PS and i-PS characteristics are shown in *Table 2*. The 60/40 (w/w) i-PS/a-PS mixtures were dissolved at 1.8 wt% total polymer concentration in dichloromethane. The solutions were cast onto cover glasses (for microscopy) or poured into shallow glass dishes (for differential scanning calorimetry (d.s.c.)). The solvent was evaporated from each sample at room temperature for one day, and the films were further dried under vacuum (10^{-4} mmHg) at room temperature for one day.

The glass transition temperature (T_g) of each dried film was measured by d.s.c. (910 DSC, Du Pont) at a heating rate of 20°C min^{-1}.

Each dried film was maintained at 240°C (higher than the melting point) for 3 min, and then the melt was rapidly quenched to the crystallization temperature by putting it in a hot-stage (Linkam TH600) set on an optical microscope stage. The time variation of the spherulite radius during isothermal crystallization was observed using a polarized optical microscope (Olympus BH-2) equipped with a TV video recording system.

For the melting point measurements, the mixtures were placed in aluminium pans (for d.s.c.) and isothermally crystallized for more than 48 h at various crystallization temperatures. The melting points were measured by d.s.c. at a heating rate of 20°C min^{-1}. The equilibrium melting temperatures were estimated from a Hoffman–Weeks plot.

0032-3861/94/26/5699-07

Table 1 The growth modes of polymer/polymer mixtures[a]

Crystalline polymer	Amorphous polymer	Growth mode	Ref.
PEO (M_w[b] = 0.13–9.9 × 10^5)	PMMA (M_w = 0.01–5.25 × 10^5)	Linear	3
PVDF (M_w = 7.0 × 10^4)	PMMA (M_w = 0.13–9.3 × 10^5)	Linear	4
i-PP (M_η[c] = 1.78 × 10^5)	a-PP (M_η = 8.7 × 10^4)	Linear	6
PCL (M_w = 3.3 × 10^4)	a-PS (M_w = 950)	Non-linear	5
i-PP (M_η = 1.78 × 10^5)	a-PP (M_n[d] = 540)	Non-linear	6
i-PS (M_η = 6.0 × 10^4)	a-PS (M_η = 4500)	Non-linear	6
i-PP (M_w = 3.5 × 10^5)	Liquid paraffin (M_w = 338)	Non-linear	7

[a] PEO = poly(ethylene oxide), PVDF = poly(vinylidene fluoride), PP = polypropylene, PCL = polycaprolactam, PS = polystyrene, PMMA = poly(methyl methacrylate)
[b] M_w = weight average molecular weight
[c] M_η = viscosity average molecular weight
[d] M_n = number average molecular weight

Table 2 Characteristics of the a-PSs and i-PS

	M_w	M_w/M_n	T_g(°C)
A300	420	1.13	−51
A1000	950	1.13	2
A5000	5200	1.03	85
F2	1.91 × 10^4	1.01	98
F4	4.3 × 10^4	1.01	100
F10	9.9 × 10^4	1.02	100
F20	1.89 × 10^5	1.04	100
F80	7.70 × 10^5	1.05	100
F126	1.30 × 10^6	1.05	100
i-PS	4.0 × 10^5	–	85

RESULTS AND DISCUSSION

Spherulite growth behaviour

Typical time variations of the spherulite radius R at a crystallization temperature T_c = 180°C are shown in *Figure 1*. As shown in *Figure 1a*, when the molecular weight M_A of a-PS is low (M_A = 420), R initially increases linearly with time and later the growth rate decreases, i.e. non-linear growth is seen[7]. As shown in *Figure 1b*, when M_A is high (M_A = 1.3 × 10^6), R increases linearly with time before contact between spherulites occurs, i.e. spherulite growth is linear. Linear growth was observed at various crystallization temperatures when M_A was high, while non-linear growth was observed for low M_A systems. The results are summarized in *Figure 2*. The dependence of M_A on the glass transition temperature (T_g) and the equilibrium melting temperature (T_m^o) is also shown in *Figure 2*. The spherulite growth mode seems to be independent of the crystallization temperature but dependent on M_A. A transition from the linear to the non-linear mode seems to occur at an M_A between 5200 and 1.91 × 10^4. Note that the molecular weight between entanglements M_e in a-PS is in this M_A range ($M_{e,A}$ = 18 700)[8]. *Figure 3* shows the M_A dependence of the spherulite growth rate G for each T_c. G was obtained from the initial slope of $R(t)$. At high temperature (T_c = 195°C), G increases steeply with increasing M_A and then starts to decrease slightly. On the other hand, at low temperatures (e.g. T_c = 150°C), G decreases with increasing M_A, attains a minimum, increases abruptly and then finally starts to decrease. Similar results have been obtained by Yeh and Lambert[9]. Particularly interesting is the existence of the minimum at low temperatures. Note that non-linear growth is seen in *Figure 2* when M_A is less than M_A at the minimum point in *Figure 3*. This suggests that the kinetics of non-linear growth are somewhat different from those of linear growth.

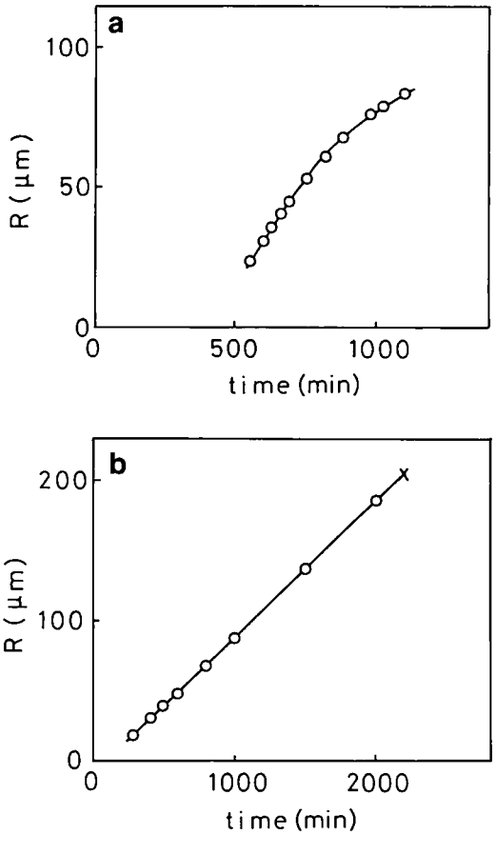

Figure 1 Time variation of the spherulite radius R: (a) 60/40 i-PS/A300; (b) 60/40 i-PS/F126

On the Keith–Padden δ parameter

In the discussion of the spherulite growth mode (non-linear or linear), it may be interesting to employ the Keith–Padden δ parameter, which describes the scale of the exclusion distance for impurities[10–13]

$$\delta = \frac{D_A^*}{G} \quad (\mu m) \tag{1}$$

where D_A^* is the tracer diffusion coefficient of the impurity. According to the recent theory of Hess *et al.*[14], D_A^* is

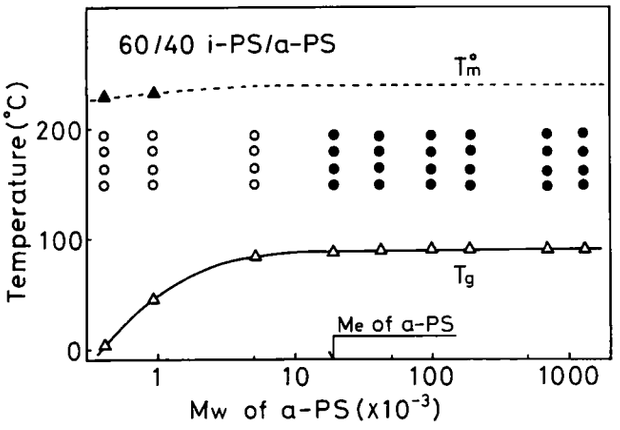

Figure 2 Equilibrium melting temperature (T_m°), glass transition temperature (T_g) and spherulite growth mode for 60/40 i-PS/a-PS mixtures as a function of a-PS molecular weight: (○) non-linear growth; (●) linear growth

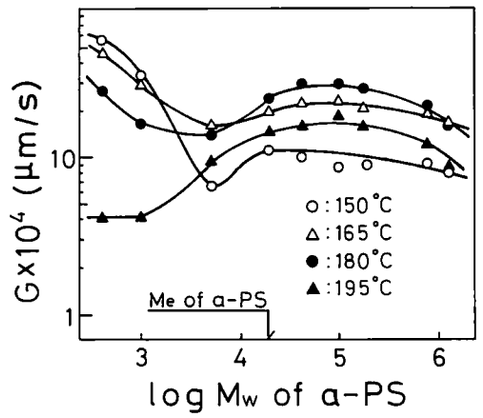

Figure 3 Plots of G for 60/40 i-PS/a-PS mixtures as a function of a-PS molecular weight for various temperatures

given by

$$D_A^* = \frac{kT_c}{\phi_A \zeta_{AA} + \phi_C \zeta_{AC}} \tag{2}$$

where ϕ_A is the volume fraction of the impurity, ϕ_C is that of the crystalline component, k is the Boltzmann constant, ζ_{AA} is the friction coefficient for A–A contact and ζ_{AC} is that for A–C contact in the mixture. Assuming that ζ_{AC} is given by the geometric mean[15], i.e. $\zeta_{AC} = (\zeta_{AA}\zeta_{CC})^{1/2}$, ζ_{CC} being the friction coefficient for C–C contact, D_A^* can be rewritten as

$$D_A^* = \frac{1}{\phi_A D_A^{-1} + \phi_C (D_A D_C)^{-1/2}} \tag{3}$$

where D_A is the self-diffusion coefficient of the impurity ($D_A = kT_c/\zeta_{AA}$) and D_C is that of the crystalline component ($D_C = kT_c/\zeta_{CC}$). On the basis of reptation theory[16,17], D_A is given by

$$D_A = D_0 P M_0 / M_A \tag{4}$$

for non-entangled systems and

$$D_A = D_0 P M_0 M_e / M_A^2 \tag{5}$$

for entangled systems, where M_0 is the segment molecular

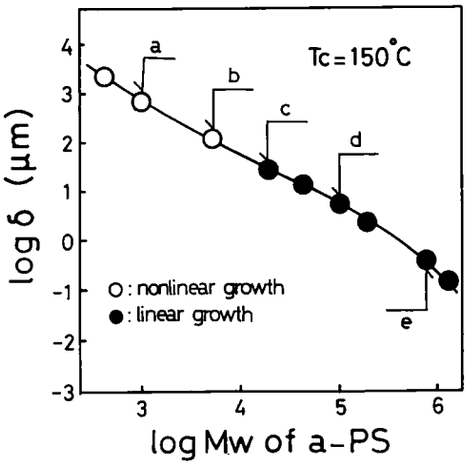

Figure 4 Plot of δ for 60/40 i-PS/a-PS mixtures as a function of a-PS molecular weight

weight, M_A is the molecular weight of the impurity, M_e is the molecular weight between entanglements in the mixture, D_0P is the segment diffusion coefficient at T_c and P is given by

$$P = \exp\left[-\frac{B}{F_g + \Delta\alpha(T_c - T_g)}\right] \tag{6}$$

where B is a constant characterizing the hole size required for the jump of a segment, F_g is the fractional free volume at T_g and $\Delta\alpha$ is the temperature coefficient of the fractional free volume. When the molecular weight M_c of the crystalline polymer is higher than M_e, D_C is given by

$$D_C = D_0 P M_0 M_e / M_C^2 \tag{7}$$

Since the values of M_e for i-PS and a-PS have already been measured by Wu ($M_{e,A} = 18\,700$ and $M_{e,C} = 28\,800$)[8], one can calculate M_e for a 60/40 i-PS/a-PS mixture as[18]

$$M_e = \left(\frac{\phi_C}{M_{e,C}} + \frac{\phi_A}{M_{e,A}}\right)^{-1} \approx 23\,700 \tag{8}$$

Employing the literature data[16,19] $D_0 = 0.41\ \mathrm{cm^2\,s^{-1}}$, $B = 0.66$, $F_g = 0.025$ and $\Delta\alpha = 8.33 \times 10^{-4}\ \mathrm{K^{-1}}$ for equations (1)–(7), we calculated the corresponding δ values. The results are shown in *Figure 4* as a function of M_A. The non-linear growth mode is seen for large δ and the linear mode for small δ. However, there is no way to predict the mode transition value of δ. One needs a new parameter to define the mode transition observed in *Figure 4*.

Originally, Keith and Padden used the δ parameter in an investigation of fibril size[10–12]. Later, Tanaka and Nishi used δ in an investigation of instability in the spherulite texture[5]. It is therefore interesting to investigate the relationship between δ and spherulite texture. Polarized optical micrographs of spherulites are shown in *Figure 5*. The micrographs in *Figures 5a–e* are of specimens crystallized at 150°C for 38 h and correspond to points a–e in *Figure 4*. As δ increases from *Figure 5e* to *Figure 5b*, the fibril size increases. However, the spherulite in *Figure 5a* with the largest δ has thinner fibrils than that in *Figure 5b*. Concerning the instability of the spherulite, on the other hand, that in *Figure 5b* is less stable than that in *Figure 5a*, even though δ is larger in

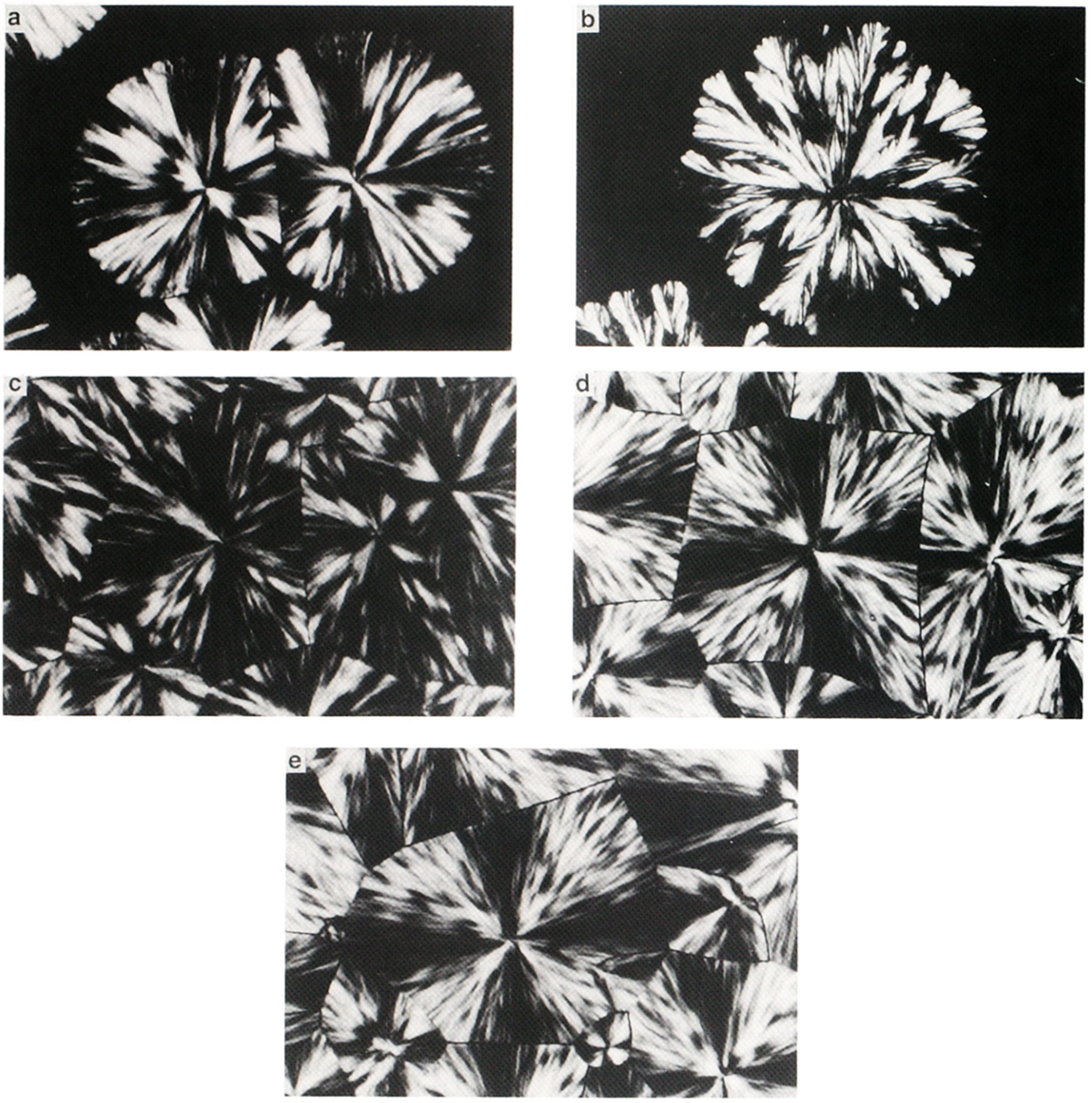

Figure 5 Polarized optical micrographs (1.8 cm = 30 μm) of spherulites crystallized at $T_c = 150$°C for 38 h: (a) $\delta = 713\ \mu$m; (b) $\delta = 134\ \mu$m; (c) $\delta = 28\ \mu$m; (d) $\delta = 5.9\ \mu$m; (e) $\delta = 0.38\ \mu$m

the latter. These unexpected results probably suggest that we have missed an important aspect of the crystallization kinetics. In this article, we would like to propose the importance of a two-step diffusion mechanism in the crystallization kinetics of polymer/diluent systems on the basis of the Hoffman–Lauritzen (H–L) theory. Before getting into the details, we will first give a short review of the H–L theory and apply it to a neat i-PS system.

Kinetics of spherulite growth in neat i-PS

According to the H–L theory[1,2], G is given by

$$G \propto \beta_g \exp\left(-\frac{K T_m^\circ}{T_c \Delta T f}\right) \tag{9}$$

and

$$\beta_g = D_T \exp\left[-\frac{U}{R_g(T_c - T_\infty)}\right] \tag{10}$$

where K is the nucleation parameter which depends on the crystallization regime, β_g is the chain mobility term, T_m° is the equilibrium melting temperature (240°C for i-PS), ΔT ($= T_m - T_c$) is the supercooling, f is the correction factor given by $2T_c/(T_m^\circ + T_c)$, R_g is the gas constant, $T_\infty = T_g - F_g/\Delta\alpha = T_g - 30$, $U = B/\Delta\alpha = 1560$ cal mol^{-1} (from Suzuki and Kovacs[19]) and D_T is the chain diffusivity which does not depend on T_c but depends on M_A and M_C.

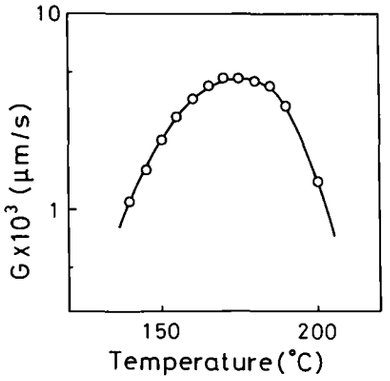

Figure 6 *G versus* T_c plot for neat i-PS

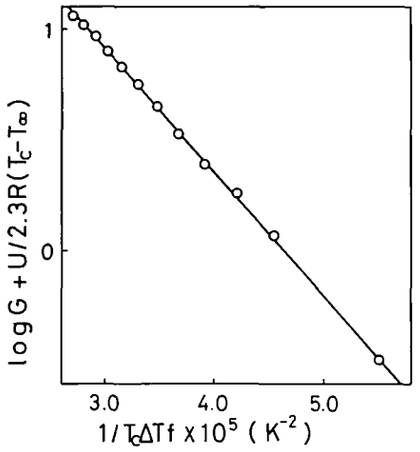

Figure 7 Plot of $\log G + U/2.3R_g(T_c - T_\infty)$ *versus* $1/T_c\Delta Tf$ for neat i-PS ($U = 1560$ cal mol^{-1}, $T_\infty = T_g - 30$)

Figure 6 shows the temperature dependence of G in neat i-PS. As expected from equations (9) and (10), G increases with increasing T_c (starting from T_g), then starts to decrease as T_c approaches T_m°. Thus, the temperature dependence is nicely interpreted by the H–L theory. If one plots $G\exp[U/R_g(T_c - T_\infty)]$ *versus* the ΔT term as in *Figure 7*, the value of K is given by the slope of the straight line. The straight line for the kinetic analysis over a wide range of T_c suggests the validity of the H–L theory. Following the Lauritzen Z test[1], the crystallization in i-PS is considered to be regime II.

Obtaining β_g *in mixtures*

From equation (9), the value of the chain mobility term β_g can be obtained from

$$\beta_g \propto G\exp\left(\frac{KT_m^\circ}{T_c\Delta Tf}\right) \tag{11}$$

The results for i-PS/a-PS mixtures are shown in *Figure 8* as a function of M_A for various temperatures. Here we have assumed that K in the blend is equal to K in neat i-PS and that growth occurs in regime II. In the low M_A region, β_g decreases with increasing M_A, attains a minimum and then increases. On the other hand, in the high M_A region, β_g decreases with increasing M_A. This implies that there is some difference in the diffusion mechanism between the low M_A and high M_A regions. The difference will be elucidated by isolating the D_T term and discussing its M_A dependence.

The value of D_T can be obtained by subtracting a further $\exp[-U/R_g(T_c - T_\infty)]$ term from the results in *Figure 8*

$$D_T \propto \frac{G}{\exp(-KT_m^\circ/T_c\Delta Tf)\exp[-U/R_g(T_c - T_\infty)]} \equiv S \tag{12}$$

The results are shown as a function of M_A in *Figure 9*. D_T hardly depends on temperature at any M_A, suggesting the validity of the assumption that the growth in the blend occurs in regime II. At low M_A D_T increases linearly with increasing M_A and at high M_A it decreases. We will discuss the M_A dependence of D_T in the high M_A region, the low M_A region and finally over the whole range of M_A.

Basically, the crystal growth process in polymers has been described as consisting of two elementary processes: the deposition of the first stem on the growth front ('secondary nucleation process') and the attachment of following stems in the chain onto the crystal surface ('surface-spreading process'). According to the H–L theory, G in regime II is mostly governed by the rate of secondary nucleation i and the rate of surface spreading g[1,20,21]

$$G \propto (ig)^{1/2} \quad \text{for } iL^2/2g \gg 1 \quad \text{(regime II)} \tag{13}$$

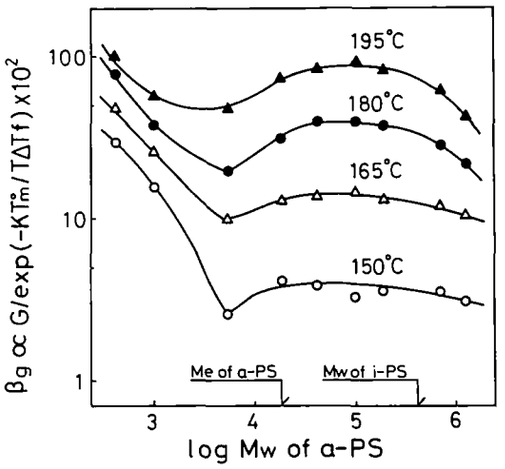

Figure 8 Plots of the β_g factor for 60/40 i-PS/a-PS mixtures as a function of a-PS molecular weight for various temperatures

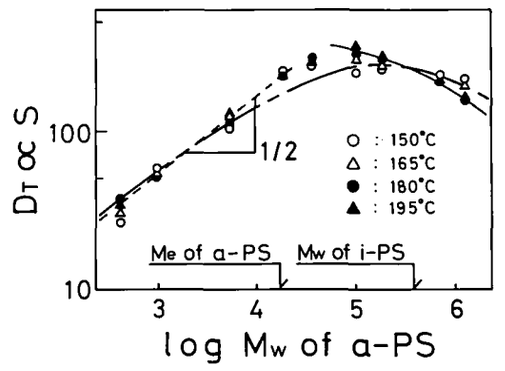

Figure 9 Plots of D_T for 60/40 i-PS/a-PS mixtures as a function of a-PS molecular weight for various temperatures: (—) calculated from equation (19); (– – –) $D_T \propto M_A^{1/2}$; (— — —) calculated from equation (27)

where L is the width of the substrate, i consists of the mobility term β_g and a supercooling term (the exponential term in equation (14)) and g consists of β_g. We define the diffusion coefficients in the surface nucleation process and the surface-spreading process as D_M and D_s, respectively. Assuming that β_g is proportional to the diffusion coefficient, i and g may be given by

$$i \propto D_M \exp\left(-\frac{KT_m^\circ}{T_c \Delta T f}\right) \tag{14}$$

and

$$g \propto D_s \tag{15}$$

From equations (13)–(15) we obtain for regime II

$$\beta_g \propto (D_M D_s)^{1/2} \tag{16}$$

For the neat crystalline polymer system, it has been assumed that there is no distinction between D_M and D_s[1,2]. However, in the mixture of crystalline polymer and amorphous polymer, the situation should be different, probably because of exclusion of amorphous polymer from the crystal growth front. In other words, diffusion in the secondary nucleation process should be controlled by two competititve processes: the attachment of crystalline polymer onto the crystal surface and the exclusion of amorphous polymer from the surface. This competitive situation can be characterized as mutual diffusion. On the other hand, the surface-spreading process may be controlled by the rate of pull-out of residual segments in the crystalline chain from the melt near the growth front. This can be characterized as self-diffusion, as in the neat system.

The mutual diffusion coefficient for a binary blend of polymers has been formulated as[22]

$$D_M = \frac{D_0 P M_0}{\phi_C M_A + \phi_A M_C} Q \tag{17}$$

where ϕ is the volume fraction and Q is the thermodynamic driving force for diffusion. We assume that Q is independent of M_A and temperature. On the other hand, D_s is the self-diffusion coefficient of the Rouse model[23]

$$D_s \propto D_0 P M_0 / M_C \tag{18}$$

From equations (12)–(18), D_T in the high M_A region can be rewritten as

$$D_T \propto S_h \equiv Q_h D_0 \left(\frac{M_0}{\phi_C M_A + \phi_A M_C} \frac{M_0}{M_C}\right)^{1/2} \tag{19}$$

where Q_h is a constant. The M_A dependence of D_T in the high M_A region in *Figure 9* is expected to be described by equation (19). The calculated result is shown by the solid line in *Figure 9*. The observed points are scattered around the solid line.

On the other hand, the M_A dependence of D_T in the low M_A region is given by $D_T \propto M_A^{1/2}$, as shown by the dashed line in *Figure 9*. As has been discussed for *Figure 2*, the growth is non-linear. The above dependence of D_T implies that a build-up of a-PS on the growth front affects the growth rate even in the initial stages. This effect can be introduced by assuming that part of the growth front is covered with the excluded a-PS, i.e.

$$D_T \propto \frac{(D_s/D_M)^{1/2}}{d^2} \equiv S_l \tag{20}$$

where d is the exclusion length, which is given by

$$d = (D_A^* \tau)^{1/2} \tag{21}$$

and

$$\tau \propto D_s^{-1} \tag{22}$$

where τ is the characteristic time required to form a crystal stem on the lamella. D_A^* and D_M in the low M_A region are described by

$$D_A^* = \frac{D_0 P M_0}{\phi_A M_A + \phi_C M_C (M_A/M_e)^{1/2}} \tag{23}$$

and

$$D_M = \frac{D_0 P M_0}{\phi_c M_e + \phi_A M_C} Q \tag{24}$$

From equations (20)–(24), S_l ($\propto D_T$) can be rewritten as

$$S_l = Q_l D_0 \frac{\phi_A M_A + \phi_C M_C (M_A/M_e)^{1/2}}{M_C} \tag{25}$$

where Q_l is a constant. When M_A is very small, equation (25) can be approximatelu rewritten as

$$S_l \propto M_A^{1/2} \tag{26}$$

This explains the $M_A^{1/2}$ power law in *Figure 9*.

S_l describes exclusion-controlled growth, while S_h describes pull-out-controlled growth. In reality, S_h and S_l compete with each other, so that an overall S may be given by a phenomenological equation

$$S = \frac{\alpha\beta S_h S_l}{\alpha S_h + \beta S_l} \tag{27}$$

where α and β are adjustable parameters. S ($\propto D_T$) for the whole range of M_A calculated from equation (27) is shown by the broken curve in *Figure 9* ($\alpha = 1.4$, $\beta = 1.2$). Thus, the M_A dependence of D_T is successfully interpreted by a two-step diffusion mechanism which involves the exclusion effect. This suggests the possibility of interpreting the mode transition discussed in *Figures 2* and *4*.

Mode transition

From equations (21) and (22), d^2 is given by

$$d^2 \propto \frac{D_A^*}{D_s} = \frac{M_C}{\phi_A M_A + \phi_C M_C (M_A/M_e)^{1/2}} = \lambda \tag{28}$$

where λ is defined as the exclusion parameter. As already discussed, a transition from the linear to the non-linear mode seems to occur at an M_A between 5200 and 1.91×10^4. Assuming that the transition occurs at the midpoint, λ_t at the transition is calculated as 2.28. Non-linear growth is expected for $\lambda > \lambda_t$ and linear growth is expected for $\lambda < \lambda_t$. In the literature[5,9] one can find experimental results on the mode transition for i-PS/a-PS mixtures with various values of M_C. In addition to the results from this work, the literature data are plotted in *Figure 10* on a map of M_C *versus* M_A. The open symbols indicate the non-linear mode while the closed symbols indicate the linear mode. The solid line in *Figure 10* was calculated from equation (28) under the assumption that λ is equal to λ_t (=2.28). The map is divided by the solid line into non-linear and linear regions, except for two of the points of Yeh and Lambert[9]. These two points may

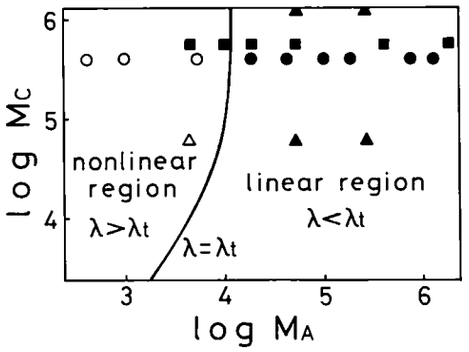

Figure 10 A map of the spherulite growth mode as a function of the molecular weights of i-PS (M_c) and a-PS (M_A) for 60/40 i-PS/a-PS mixtures: (○, ●) present work; (■) Yeh and Lambert[9]; (△, ▲) Keith and Padden[6,10,11]. The open symbols represent non-linear growth and the closed symbols represent linear growth

be classified as belonging to the linear mode because the limited crystallization time was probably insufficient to reveal the non-linearity. In any case, we believe that λ is a new kinetic parameter which characterizes the spherulite growth mode.

REFERENCES

1 Lauritzen Jr, J. I. and Hoffman, J. D. *J. Appl. Phys.* 1973, **44**, 4340
2 Hoffman, J. D., Frolen, L. J., Ross, G. S. and Lauritzen Jr, J. I. *J. Res. Natl Bur. Stand., Sect. A* 1975, **79**, 671
3 Alfonso, G. C. and Russell, T. P. *Macromolecules* 1986, **19**, 1143
4 Saito, H., Okada, T., Hamane, T. and Inoue, T. *Macromolecules* 1991, **24**, 4446
5 Tanaka, H. and Nishi, T. *Phys. Rev. Lett.* 1985, **55**, 1102
6 Keith, H. D. and Padden Jr, F. J. *J. Appl. Phys.* 1964, **35**, 1286
7 Okada, T., Saito, H. and Inoue, T. *Macromolecules* 1990, **23**, 3865
8 Wu, S. *J. Polym. Sci., Polym. Phys. Edn* 1989, **27**, 723
9 Yeh, G. S. Y. and Lambert, S. L. *J. Polym. Sci. A-2* 1972, **10**, 1183
10 Keith, H. D. and Padden Jr, F. J. *J. Appl. Phys.* 1964, **35**, 1270
11 Keith, H. D. and Padden Jr, F. J. *J. Appl. Phys.* 1963, **34**, 2409
12 Keith. H. D. *J. Polym. Sci. A* 1964, **2**, 4339
13 Stein, R. S., Khambatta, F. B., Warner, F. P., Russell, T., Escala, A. and Balizer, E. *J. Polym. Sci., Polym., Symp. Edn* 1978, **63**, 313
14 Hess, W., Nagele, G. and Akcasu, A. Z. *J. Polym. Sci., Polym. Phys. Edn* 1990, **28**, 2233
15 Wu, S. *J. Polym. Sci., Polym. Phys. Edn* 1987, **25**, 2511
16 Fleischer, G. *Polym. Bull.* 1984, **11**, 75
17 Doi, M. and Edwards, S. F. 'The Theory of Polymer Dynamics', Oxford University Press, New York, 1986, Ch. 6
18 Wu, S. *J. Polym. Sci., Polym. Phys. Edn* 1987, **25**, 557
19 Suzuki, T. and Kovacs, A. J. *Polym. J.* 1970, **1**, 82
20 Point, J. J. and Villers, D. *J. Cryst. Growth* 1991, **114**, 228
21 Toda, A. *Colloid. Polym. Sci.* 1992, **270**, 667
22 Brochard, F., Jouffroy, J. and Levinson, P. *Macromolecules* 1983, **16**, 1638
23 Hoffman, J. D. and Miller, R. L. *Macromolecules* 1988, **21**, 3038